

See discussions, stats, and author profiles for this publication at: <https://www.researchgate.net/publication/234988187>

# Statistical mechanics of small chain molecules in liquids. I. Effects of liquid packing on conformational structures

ARTICLE *in* THE JOURNAL OF CHEMICAL PHYSICS · APRIL 1978

Impact Factor: 2.95 · DOI: 10.1063/1.436284

---

CITATIONS

143

---

READS

85

3 AUTHORS, INCLUDING:



Lawrence R. Pratt

Tulane University

203 PUBLICATIONS 9,031 CITATIONS

SEE PROFILE

## Statistical mechanics of small chain molecules in liquids. I. Effects of liquid packing on conformational structures

Lawrence R. Pratt, C. S. Hsu, and David Chandler

Citation: *J. Chem. Phys.* **68**, 4202 (1978); doi: 10.1063/1.436284

View online: <http://dx.doi.org/10.1063/1.436284>

View Table of Contents: <http://jcp.aip.org/resource/1/JCPSA6/v68/i9>

Published by the [American Institute of Physics](#).

---

### Additional information on J. Chem. Phys.

Journal Homepage: <http://jcp.aip.org/>

Journal Information: [http://jcp.aip.org/about/about\\_the\\_journal](http://jcp.aip.org/about/about_the_journal)

Top downloads: [http://jcp.aip.org/features/most\\_downloaded](http://jcp.aip.org/features/most_downloaded)

Information for Authors: <http://jcp.aip.org/authors>

## ADVERTISEMENT



**Goodfellow**  
metals • ceramics • polymers • composites  
70,000 products  
450 different materials  
**small quantities fast**  
[www.goodfellowusa.com](http://www.goodfellowusa.com)

# Statistical mechanics of small chain molecules in liquids. I. Effects of liquid packing on conformational structures<sup>a)</sup>

Lawrence R. Pratt,<sup>b)</sup> C. S. Hsu,<sup>c)</sup> and David Chandler<sup>d)</sup>

School of Chemical Sciences, University of Illinois, Urbana, Illinois 68101  
(Received 14 December 1977)

When a chain molecule can be viewed as a collection of overlapping spherical groups, the effect of a solvent on the conformational structure of the chain molecule is described by the distribution function for the cavity particles associated with the spherical groups. This article discusses the calculation of the cavity distribution function for *n*-butane dissolved in various apolar solvents: the liquids carbon tetrachloride, *n*-butane, and *n*-hexane. We consider the common picture where the CH<sub>3</sub> and CH<sub>2</sub> groups in *n*-butane are simple spheres. For that model, the cavity distribution function is a four-point correlation function. We find that the superposition approximation for the four-point function, while qualitatively correct, overestimates the effects of the solvent. An alternative scheme, which is called the two cavity model, yields results that agree quantitatively with a computer simulation study of liquid *n*-butane. We find that a solvent medium produces significant shifts in the conformational equilibrium of *n*-butane from that found in the gas phase. This phenomenon is the result of the nature of the local packing of solvent molecules neighboring the solute species under investigation. The conformational equilibrium is sensitive to this packing. The bulk packing fractions (molecular density times the volume of the molecule) of the liquids CCl<sub>4</sub> and C<sub>4</sub>H<sub>10</sub> are nearly identical. Even so there are noticeable differences between the intramolecular structure of *n*-butane in liquid carbon tetrachloride and in the neat liquid. Previous ideas on conformational equilibria have ignored the importance of steric (i.e., liquid packing) effects, and have assumed that solvent shifts in conformational structures can be attributed entirely to dielectric effects. Our calculations show that this assumption is wrong. The *n*-butane molecule contains no significantly polar groups, yet solvent media produce substantial shifts. For example, the *trans*-*gauche* equilibrium constant,  $x_g/x_t$ , for *n*-butane in the gas phase at room temperature is roughly 0.5, while we find it is about 1.0 when *n*-butane is dissolved in liquid CCl<sub>4</sub> at the same temperature and 1 atm pressure. We discuss why the phenomenon has been overlooked, and suggest experiments to document its existence.

## I. INTRODUCTION

In a recent pair of articles,<sup>1,2</sup> we developed a rigorous statistical mechanical theory for describing conformational structures of nonrigid molecules dissolved in liquid solvents. To apply the theory, approximations must be made. The purpose of this paper is to describe some of the possible approximations. Many of the ideas we explore have already been touched upon in our earlier study of the hydrophobic effect.<sup>3</sup> However, the emphasis in that work was on the properties peculiar to aqueous solutions. In the present article, we consider the conformational structure of *n*-butane molecules in various nonassociated liquid solvents.

The motivation for this study is twofold. First, traditional treatments of the effects of condensed phases on intramolecular structures have ascribed solvent effects entirely to the dielectric energetics of changing low order moments of the electric charge distributions of nonrigid molecules.<sup>4</sup> Of course, *n*-butane has no significant polarity. By considering *n*-butane we show that even without electrostatic contributions, the local packing of solvent and solute species gives rise to an appreciable

change in the intramolecular distribution from that in the gas phase. For molecules containing polar groups, it is undoubtedly true that electrostatic contributions also play a role. But the role of steric effects seems to be ignored in the literature, perhaps because a theory for the effects has not been previously available. We believe that the traditional treatments of molecular conformational structures in condensed phases must be critically re-examined in order to accommodate the results we present here. There also seems to be a need for more extensive experimental studies of conformational equilibria in condensed phases. As we will discuss, the standard interpretation of conformational equilibria considers only the temperature dependence of the equilibrium constant and neglects the density (or pressure) dependence. With this approach, one observes a mean field electrostatic contribution and usually fails to see anything about the steric contribution. An entire phenomenon is usually overlooked.

A second reason for studying the intramolecular structure of *n*-butane in nonassociated solvents is that for these solvents the calculation of equilibrium correlation functions is relatively straightforward and noncontroversial. Hence, we are able to focus clearly on the statistical mechanical problems associated with the intramolecular structure of the solute molecule.

In Sec. II, the basic theory for *n*-butane is reviewed. The justifications of the principal equations are not discussed because a full treatment can be found in Refs. 1 and 2. In Sec. III, we consider *n*-butane dissolved in liquid carbon tetrachloride. Two approximations are explored. One is a superposition approximation for the

<sup>a)</sup>This research has been supported by the National Science Foundation and by the donors of the Petroleum Research Fund as administered by the American Chemical Society.

<sup>b)</sup>Present address: Department of Chemistry, Harvard University, Cambridge, MA 02138.

<sup>c)</sup>Present address: Solid State Sciences Division, Argonne National Laboratory, Argonne, IL 60432.

<sup>d)</sup>On leave for the 1977-78 academic year at the Department of Chemistry, Columbia University, New York, NY 10027.

intramolecular structure, while the other is a scheme we call the two cavity model. Both yield qualitatively similar results. But we argue that the two cavity model is the more accurate of the two. This assessment is bolstered in Sec. IV, where the two cavity model is used to study *n*-butane in liquid *n*-butane. We find that our result for the *trans*-*gauche* equilibrium constant compares favorably with that found from the Ryckaert-Bellemans<sup>5</sup> computer simulation of *n*-butane.

When studying *n*-butane dissolved in *n*-butane, there is a self-consistency aspect to the calculations. The intramolecular structure of *n*-butane depends on the intermolecular structure of the surrounding liquid solvent; and the intermolecular structure clearly depends upon the intramolecular correlations of the solvent molecules because these correlations determine the shape of the solvent molecules. The self-consistency aspect of the problem is attacked by employing the RISM theory<sup>6</sup> for the intermolecular structure. We consider in Sec. IV the behavior of *n*-butane in the solvents liquid *n*-butane and liquid *n*-hexane. We find that the conformational equilibrium of *n*-butane in both of these solvents are similar and significantly different than the equilibrium for *n*-butane in the gas phase. However, the packing of the *n*-butane and *n*-hexane solvents does not affect the *n*-butane intramolecular structure as much as does the packing of liquid carbon tetrachloride.

This article is concluded in Sec. V with a discussion of the experimental significance of our calculations. To make the application and thus experimental test of our theory particularly convenient, the correlation functions that are needed when using the two cavity model are tabulated in the Appendix.

## II. THEORY

The intramolecular structure of a nonrigid molecule can be described with the intramolecular distribution function,  $s_M(1_M)$ , where  $1_M = (\gamma_{1M}^{(1)}, \dots, \gamma_{1M}^{(\alpha)}, \dots, \gamma_{1M}^{(n_M)})$  denotes the positions of all the  $n_M$  atoms (or spherical groups) in molecule 1 of type  $M$ . For *n*-butane, a lot of this information is trivial. The only appreciable conformational degree of freedom is the dihedral angle  $\phi$ .<sup>7</sup> See Fig. 1. Its distribution is

$$s(\phi) = \langle \delta(\phi - \phi[1_M]) \rangle \\ = V^{-1} \int d1_M s_M(1_M) \delta(\phi - \phi[1_M]), \quad (2.1)$$

where the pointed brackets stand for the equilibrium ensemble average, and  $V$  is the volume of the container.

In the gas phase,  $s(\phi)$  is given by

$$s^{(0)}(\phi) = \exp[-\beta V(\phi)] \left( \int_{-\pi}^{\pi} d\phi' \exp[-\beta V(\phi')] \right)^{-1}, \quad (2.2)$$

where  $\beta^{-1} = k_B T$ , the superscript 0 indicates a gas phase result, and  $V(\phi)$  is the potential which describes the intramolecular energetics of altering  $\phi$ . [The reader may verify that the Jacobian for transforming from the partially constrained atomic (or interaction site) coordinates to  $\phi$  is unity.] Scott and Scheraga<sup>8</sup> have proposed the following semiempirical model for  $V(\phi)$ :

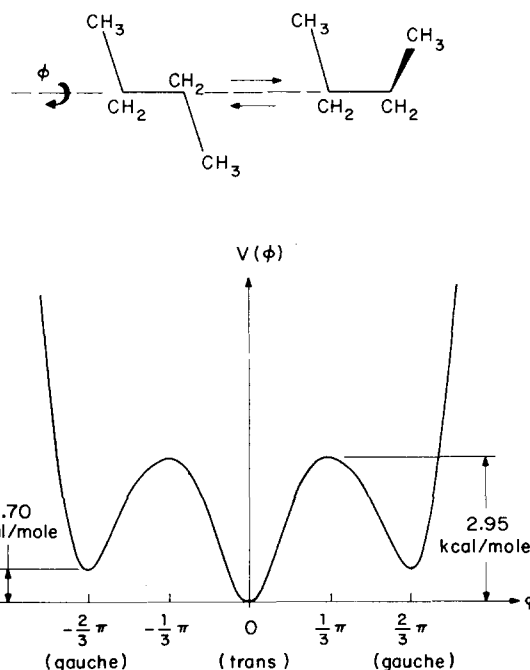


FIG. 1. *Trans*-*gauche* equilibrium and the Scott-Scheraga potential,  $V(\phi)$ , for *n*-butane.

$$V(\phi)/k_B = (1.116 + 1.462 \cos \phi - 1.578 \cos^2 \phi - 0.368 \cos^3 \phi \\ + 3.156 \cos^4 \phi - 3.788 \cos^5 \phi) 10^3 \text{ } ^\circ\text{K}, \quad (2.3)$$

which we adopt throughout this article. There are three stable minima in  $V(\phi)$ . See Fig. 1. The lowest energy state is the *trans* conformer,  $\phi = 0^\circ$ . The other two stable states are *gauche* conformers,  $g^+$  and  $g^-$ , located at  $\phi \approx \pm 120^\circ$ . The *cis* state, at  $\phi = 180^\circ$ , has a very high and unstable energy.

Since conformational rearrangements in liquids involve the displacement of solvent molecules, the ability of the solvent to literally digest a particular conformational species must be accounted for. The exact condensed phase result for  $s(\phi)$  is<sup>1,2</sup>

$$s(\phi) = s^{(0)}(\phi) y^*(\phi) \left( \int_{-\pi}^{\pi} d\phi' s^{(0)}(\phi') y^*(\phi') \right)^{-1}, \quad (2.4)$$

where  $y^*(\phi)$  is the cavity distribution function for *n*-butane when the atomic configuration conforms to a structure with dihedral angle  $\phi$ . The relationship between  $s(\phi)$  and  $y^*(\phi)$  is derived<sup>1,2</sup> by viewing nonrigid molecules like *n*-butane as collections of spherical *cavity* particles. These hypothetical particles are defined so that they are nearly identical to real particles. Cavities are distinguished solely by the fact that they do not interact with each other. However, cavities interact with real particles just as if cavities were real particles. [In the theory of simple one component fluids, a cavity distribution would correspond to the radial distribution function,  $g(r)$ , after the direct Boltzmann factor containing the pair interaction,  $u(r)$ , has been removed from it; i. e., the quantity  $g(r) \exp[+\beta u(r)]$  is a cavity distribution function.] Direct (intramolecular) interactions are not present in  $y^*(\phi)$  since direct intramolecular energetics are properly accounted for with  $V(\phi)$ .

According to Eq. (2.4), the effects of condensed phase environments are known once the cavity distributions are known. For example, the *trans-gauche* mole fraction equilibrium constant for *n*-butane,

$$K = x_g/x_t, \quad (2.5)$$

is given by

$$K = 2 \int_g d\phi s(\phi) \left( \int_t d\phi s(\phi) \right)^{-1} \\ = 2 \int_g d\phi s^{(0)}(\phi) y^*(\phi) \left( \int_t d\phi s^{(0)}(\phi) y^*(\phi) \right)^{-1} \quad (2.6)$$

$$\approx (x_g^{(0)}/x_t^{(0)}) (y_g^*/y_t^*). \quad (2.7)$$

The subscript *g* on the integration symbol indicates that the integration is confined to those values of  $\phi$  associated with one of the two *gauche* states (e.g.,  $\pi/2 < \phi < \pi$ ). The *t* subscript denotes the *trans* region. The factor of 2 comes about because there are two *gauche* states,  $g^+$  and  $g^-$ . The quantities  $y_g^*$  and  $y_t^*$  are the values of  $y^*(\phi)$  near the *gauche* and *trans* peaks of  $s^{(0)}(\phi)$ . It is assumed in passing from Eq. (2.6) to (2.7) that  $s^{(0)}(\phi)$  is highly localized compared to the variation of  $y^*(\phi)$ . [Numerical work which employs the Scott-Scheraga model for  $V(\phi)$  indicates that Eq. (2.7) is accurate to within 2%.]

Of course, the calculation of  $y^*(\phi)$  is not necessarily simple even for *n*-butane dissolved in a solvent like carbon tetrachloride. To understand the nature of the problem, consider a common picture of *n*-butane in which the butane molecule is composed of four overlapping spherical cavities centered on each of the carbon atoms. With that model,  $-k_B T \ln y^*(\phi)$  is the reversible work (at constant  $T$ ,  $V$ , and  $N$ ) to bring the four cavities which are initially infinitely far apart in the liquid solvent to a mutual configuration which corresponds to an *n*-butane molecule with dihedral angle  $\phi$ . In other words,

$$y^*(\phi) = y_M^*[1_M(\phi)] \quad (2.8)$$

is a four-point correlation function. One simple approximation to multipoint distributions is the superposition approximation

$$y_M^*(1_M) \approx \sum_{\alpha > \gamma=1}^{n_M} y_{\alpha\gamma}^*(|\mathbf{r}_{1M}^{(\alpha)} - \mathbf{r}_{1M}^{(\gamma)}|), \quad (2.9)$$

which reduces the problem to that of calculating correlation functions for pairs of cavities. Such a calculation is not difficult. However, we have found in our study of the hydrophobic effect<sup>3</sup> that under certain circumstances the superposition approximation can incur significant qualitative errors. Hence it is possible that some other scheme to calculate  $y^*(\phi)$  is required.

This possibility is examined in the next section when we compare a calculation which employs the superposition approximation with one that uses an alternative method. The alternative is a two cavity model for *n*-butane. To describe it, let us initially assume that *n*-butane is composed of four spherical cavities. For definiteness, we take the Ryckaert-Bellemans model<sup>5</sup> which assigns Lennard-Jones potentials to each cavity with the length and energy parameters  $\sigma_{LJ} = 3.92$  Å and  $\epsilon_{LJ} = 84$  °K. At any given temperature, we can assign

TABLE I. Effective hard sphere diameters.

Group	Temperature (°K)	Diameter (Å)
CH <sub>3</sub> , CH <sub>2</sub>	283	3.74 <sup>a</sup>
	274	3.77 <sup>a</sup>
CCl <sub>4</sub>	283	5.27 <sup>b</sup>
C <sub>2</sub> H <sub>5</sub>	283	4.36 <sup>c</sup>
	274	4.39 <sup>c</sup>
C <sub>4</sub> H <sub>10</sub>	274	5.25 <sup>d</sup>

<sup>a</sup>Computed from the Verlet-Weis Table XII, Ref. 24, using the Ryckaert-Bellemans Lennard-Jones parameters, Ref. 5.

<sup>b</sup>Taken from the rough hard sphere model for the diffusion constant of liquid carbon tetrachloride, Ref. 11.

<sup>c</sup>Computed from Eq. (2.10) using the effective diameters for CH<sub>3</sub> and CH<sub>2</sub> listed above.

<sup>d</sup>Computed from Eq. (4.7) using the effective diameters for CH<sub>3</sub> and CH<sub>2</sub> listed above.

an effective hard sphere diameter  $\sigma$  to these Lennard-Jones interactions by employing the standard procedures of perturbation theory<sup>9,10</sup> and as far as the medium is concerned view *n*-butane as four hard sphere cavities. Table I gives values of effective diameters for hard sphere cavities associated with various groups at a few temperatures. In our superposition approximation calculation of  $y^*(\phi)$ ,  $y_{\alpha\gamma}^*(r)$  is a hard sphere cavity distribution for two cavities of diameter  $\sigma$ .

In the two cavity model, we replace the four hard sphere cavities with a pair of cavities. The centers of these two cavities are located at the midpoints of the outer C-C bonds, and their diameter  $d$  is chosen so that the volume  $(\pi/6)d^3$  matches the volume of an ethyl group which each of the two hard sphere cavities represents. Thus,

$$d = \sigma [1 + \frac{3}{2}(L/\sigma) - \frac{1}{2}(L/\sigma)^3]^{1/3}, \quad (2.10)$$

where  $L$  is the C-C bond length. See Fig. 2. Since in this model *n*-butane is viewed as two hard sphere ethyl cavities, the calculation of  $y^*(\phi)$  reduces to a calculation of the pair distribution for cavities with diameter  $d$ .

The calculations presented in the next section show that both the superposition approximation and the two cavity model yield qualitatively similar results. However, the two methods differ quantitatively, and the results of Sec. IV indicate that the two cavity model is the more accurate approximation.

### III. NORMAL BUTANE IN LIQUID CARBON TETRACHLORIDE: COMPARISON OF SUPERPOSITION AND TWO CAVITY APPROXIMATIONS

For the purpose of describing solvent effects on the conformational structure of *n*-butane, it is probably adequate to model liquid carbon tetrachloride as a hard sphere solvent. The effective hard sphere diameter of the carbon tetrachloride can be taken from the rough hard sphere model study of the diffusion constant.<sup>11</sup> At  $T = 283$  °K, a satisfactory fit to the experimental diffusion data was obtained with a hard sphere diameter of 5.27 Å. At 1 atm pressure and 283 °K, the density of

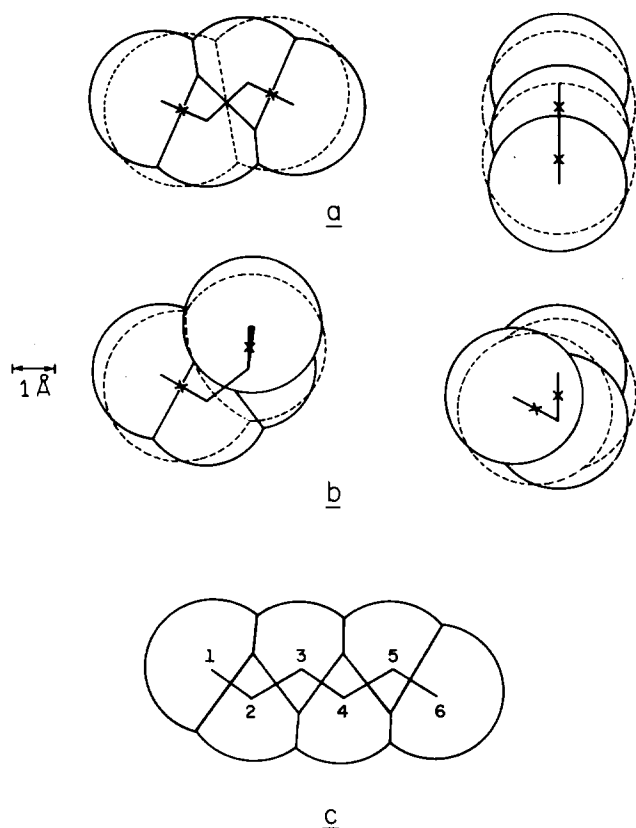


FIG. 2. Space filling models of *n*-butane and *n*-hexane. (a) Views of *n*-butane in *trans* state. (b) Views of *n*-butane in *gauche* state. The solid lines show the four cavity model, and the dashed lines show the associated two cavity model superimposed. (c) Six cavity model of *n*-hexane in the completely extended state with the carbon atoms numbered sequentially.

liquid carbon tetrachloride is<sup>12</sup>  $\rho_{\text{CCl}_4} = 6.303 \times 10^{-3} / \text{\AA}^3$ . Thus, to apply the superposition approximation at this thermodynamic state we use

$$y_{\alpha\gamma}^*(r) = y_{\text{HS}}(r; 3.74 \text{ \AA}, 5.27 \text{ \AA}; 6.30 \times 10^{-3} / \text{\AA}^3), \quad (3.1)$$

where  $y_{\text{HS}}(r; \sigma, \sigma_s; \rho_s)$  is the pair distribution for two hard sphere cavities of diameter  $\sigma$  immersed at infinite dilution in a solvent of hard spheres with diameter  $\sigma_s$  at a density  $\rho_s$ .

The calculation of hard sphere cavity pair distribution functions has been discussed by Grundke and Henderson.<sup>13</sup> However, the method they develop for the calculation of these functions fails in the limit of infinite dilution of one of the components. The Appendix describes how we modify the Grundke and Henderson method.

The cavity distributions tabulated in the Appendix and the Scott-Scheraga model for  $V(\phi)$  are combined with Eqs. (3.1), (2.9), and (2.4) to form the superposition approximation for  $s(\phi)$ . The result of this calculation is shown in Fig. 3. Notice that the calculation predicts a large shift from the ideal gas  $s^{(0)}(\phi)$  which favors *trans* over *gauche* states by a ratio of 2 to 1. The calculation of the equilibrium constant from Eq. (2.6) gives  $K = 1.47$ . The ideal gas result for the Scott-Scheraga model is  $K^{(0)} = 0.502$ . As discussed in Ref.

3, one expects the superposition approximation to overestimate the effects of the dense liquid medium on the intramolecular structure of the *n*-butane solute. To examine the possible extent of the overestimation we now consider the two cavity model.

The diameter of one of the cavities in the two cavity model is computed from Eq. (2.10) to be  $d = 4.36 \text{ \AA}$  at  $T = 283.2^\circ \text{K}$ . Thus, this model takes

$$y^*(\phi) = y_{\text{HS}}(r_{xx}[\phi]; 4.36 \text{ \AA}, 5.27 \text{ \AA}; 6.30 \times 10^{-3} / \text{\AA}^3), \quad (3.2)$$

where  $r_{xx}[\phi]$  is the distance between the midpoints of the outer C-C bonds when an *n*-butane molecule is in a configuration corresponding to the dihedral angle  $\phi$ . The two cavity model result for  $s(\phi)$  is obtained by combining Eq. (3.2) with Eq. (2.4). The result is graphed in Fig. 3. It is in qualitative agreement with the superposition approximation. However, the two cavity model predicts a smaller shift from the ideal gas behavior. The equilibrium constant with the two cavity model is  $K = 0.988$ , which should be compared with the ideal gas result of 0.502.

In the next section we compare our calculations with those of a computer simulation of liquid *n*-butane. The results presented there indicate that the two-cavity model provides a very accurate estimate of  $s(\phi)$ .

#### IV. NORMAL-BUTANE IN THE LIQUIDS *n*-BUTANE AND *n*-HEXANE

In the previous section we studied the intramolecular structure of *n*-butane when it is dissolved in a liquid composed of fairly round and rigid molecules. We now consider solvents made up of small chain molecules. The object is to discover how important it is to include a detailed description of the shape of the solvent molecules when calculating the intramolecular structure of the solute species. The RISM integral equation<sup>6</sup> provides a convenient and reliable theory<sup>14</sup> for computing

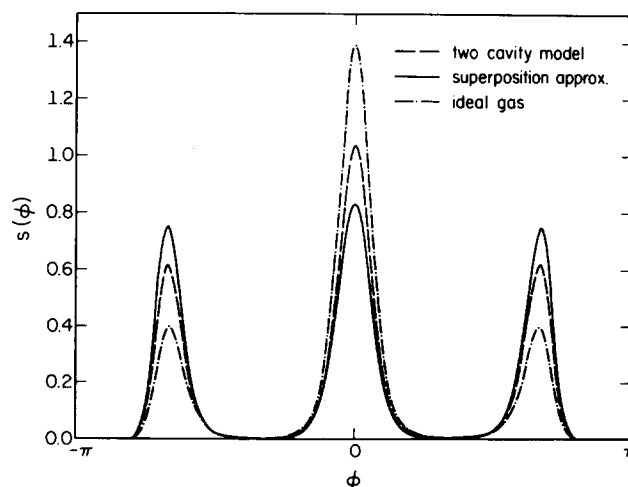


FIG. 3. Intramolecular distribution,  $s(\phi)$ , for *n*-butane at 283.2 °K. The solid and dashed lines are for *n*-butane dissolved in liquid carbon tetrachloride at 1 atm pressure. The former uses the superposition approximation described in the text, the latter uses the two cavity model. The dash-dot-dash line refers to *n*-butane in the gas phase.

the intermolecular structure of dense fluids composed of nonspherical molecules. To investigate the importance of molecular shape, the solvent is treated with the RISM equation. The results obtained in that way are then compared with those obtained when the solvent is modeled as an appropriately chosen hard sphere solvent.

We begin by first considering liquid *n*-butane as the solvent. If the *n*-butane molecules were actually rigid, application of the RISM equation to the determination of the intermolecular structure of liquid *n*-butane would be fairly straightforward. In addition to the van der Waals diameters associated with the interaction sites, one must specify the intramolecular structure by determining the lengths  $L_{\alpha\gamma}$  between each pair of sites in this molecule. The rigid molecule contracted pair intramolecular distribution functions,

$$s_{\alpha\gamma}^{(2)}(r) = [4\pi L_{\alpha\gamma}^2]^{-1} \delta(r - L_{\alpha\gamma}), \quad (4.1)$$

then appear as input in the computational procedure.<sup>14,15</sup> In applying the RISM equation to a liquid composed of nonrigid molecules the determination of  $s_{\alpha\gamma}^{(2)}(r)$  is, of course, less straightforward. The  $s_{\alpha\gamma}^{(2)}(r)$  are no longer necessarily delta functions, and they depend on the intermolecular structure (and thus on the thermodynamic state variables). However, if the  $s_{\alpha\gamma}^{(2)}(r)$  for the nonrigid molecules were known beforehand, the computational procedure would be the same as for the rigid molecule case. One expects that an efficient iteration scheme would suffice to determine the  $s_{\alpha\gamma}^{(2)}(r)$  and the intermolecular correlation functions. An initial estimate of the  $s_{\alpha\gamma}^{(2)}(r)$  would allow calculation of initial results for the intermolecular correlation functions. These correlation functions may be used to calculate cavity distribution functions, and hence a second estimate of  $s_{\alpha\gamma}^{(2)}(r)$ . For liquid *n*-butane, we find that such a procedure is essentially convergent in just one iteration when the gas phase  $s_{\alpha\gamma}^{(2)}(r)$  is used as the initial guess.

The results obtained for the intermolecular correlation functions by this procedure are reported elsewhere.<sup>16</sup> In order to determine the  $s_{\alpha\gamma}^{(2)}(r)$  appropriate to *n*-butane in a dense liquid, we require the cavity distribution function for hard sphere cavities dissolved at infinite dilution in liquid *n*-butane. However, the published RISM calculations have not treated mixtures. Furthermore, the straightforward extension of the published numerical procedures to mixtures results in a loss of accuracy in the determination of the cavity distribution functions when the limit of infinite dilution is required. Therefore, we reformulate the RISM theory explicitly for the case of a hard sphere solute dissolved at infinite dilution in a molecular liquid. The result is very similar in form to the theory presented in Ref. 3 to study the hydrophobic effect.

We begin our analysis of the RISM theory for infinitely dilute solutions of hard spheres in a molecular liquid by introducing the correlation functions associated with the solute. We designate the spherical solute as an A molecule. We then wish to calculate  $g_{AA}(r)$  and  $g_{A\alpha}(r)$ . Here,  $\alpha$  indexes the interaction sites which compose a solvent molecule. These distribution functions are de-

fined in the usual way, e.g.,  $\rho_s g_{A\alpha}(r)$  is the probability density for observing a site  $\alpha$  at position  $\mathbf{r}$  given that an A molecule is located at the origin. The molecular density of solvent molecules is denoted by  $\rho_s$ . If we study the quantities  $h_{A\alpha}(r) = g_{A\alpha}(r) - 1$ , and  $h_{AA}(r) = g_{AA}(r) - 1$ , then in the limit of infinite dilution we may write within the RISM approximation<sup>6</sup>

$$h_{A\alpha}(r - r') = c_{A\alpha}(r - r') + \sum_{\gamma} \int d\mathbf{r}'' c_{A\gamma}(|\mathbf{r} - \mathbf{r}''|) \times \{s_{\gamma\alpha}^{(2)}(|\mathbf{r}'' - \mathbf{r}'|) + \rho_s h_{\gamma\alpha}(|\mathbf{r}'' - \mathbf{r}'|)\}, \quad (4.2a)$$

and

$$h_{AA}(r) = c_{AA}(r) + \rho_s \sum_{\gamma} \int d\mathbf{r}'' c_{A\gamma}(|\mathbf{r} - \mathbf{r}''|) h_{\gamma A}(|\mathbf{r}'' - \mathbf{r}'|). \quad (4.2b)$$

Here  $h_{\alpha\gamma}(r)$  is the site-site correlation function for the pure molecular fluid. Equations (4.2a) and (4.2b) represent a slight generalization of Eqs. (2.26) in Ref. 3.

In order to obtain a RISM theory predictions for  $h_{A\alpha}(r)$  and  $h_{AA}(r)$ , we first calculate the  $h_{\alpha\gamma}(r)$  for an initial guess of  $s_{\alpha\gamma}^{(2)}(r)$ . We then use the RISM approximation,

$$\begin{aligned} c_{A\alpha}(r) &= 0 & r > \sigma_{A\alpha} = \frac{1}{2}(\sigma_A + \sigma_{\alpha}), \\ c_{AA}(r) &= 0 & r > \sigma_A, \end{aligned} \quad (4.3)$$

together with the exact relations

$$\begin{aligned} g_{A\alpha}(r) &= 0 & r < \sigma_{A\alpha}, \\ g_{AA}(r) &= 0 & r < \sigma_A, \end{aligned} \quad (4.4)$$

to close Eqs. (4.2). Equations (4.2)–(4.4) are conveniently solved by studying the functional

$$\begin{aligned} I &= \hat{c}_{A\alpha}(0) + \sum_{\alpha\gamma} [2(2\pi)^3]^{-1} \int d\mathbf{k} \hat{c}_{A\alpha}(k) \hat{s}_{\alpha\gamma}^{(2)}(k) \hat{c}_{\gamma A}(k) \\ &+ \sum_{\alpha\gamma} \rho_s [2(2\pi)^3]^{-1} \int d\mathbf{k} \hat{c}_{A\alpha}(k) \hat{h}_{\alpha\gamma}(k) \hat{c}_{\alpha A}(k), \end{aligned} \quad (4.5)$$

where the carets denote the Fourier transform. We note that

$$\delta I / \delta c_{A\alpha}(\mathbf{r}) = g_{A\alpha}(r) = 0 \quad r < \sigma_{A\alpha}. \quad (4.6)$$

The  $c_{A\alpha}(r)$  are expanded in a set of polynomials, and the expansion coefficients are determined by solving Eq. (4.6). Once the  $c_{A\alpha}(r)$ , and thus  $h_{A\alpha}(r)$ , are determined, Eq. (4.2) is then used to calculate  $h_{AA}(r)$ .

An example of the  $g_{AA}(r)$  thus obtained is shown in Fig. 4. This  $g_{AA}(r)$  was calculated in anticipation of the application of the two cavity model to the calculation of  $s(\phi)$  at 274° K. At this temperature the effective hard sphere interaction associated with the Lennard-Jones interaction has diameter 3.77 Å. With this value, the diameter of the individual cavities in the two cavity model is 4.39 Å. The  $g_{AA}(r)$  in Fig. 4 corresponds to these choices of hard sphere diameters.

To analyze the importance of the shape of the solute molecules, we also show in Fig. 4 the  $g_{AA}(r)$  which is obtained from a simple hard sphere model of the hydrocarbon solvent. This model is a packing fraction theory. The *n*-butane solvent molecules are replaced with hard spheres of diameter  $\sigma_s$  given by

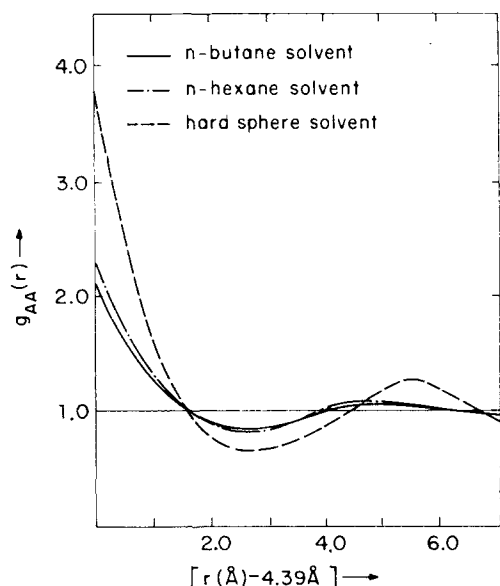


FIG. 4. Radial distribution function for two hard spheres of diameter 4.39 dissolved at infinite dilution in various solvents. The solid line is for liquid *n*-butane solvent as calculated with the RISM theory for intermolecular correlations. The dashed line is what would be found for a solvent composed of hard spheres where the molecular density is the same as that for liquid *n*-butane at room temperature and 1 atm pressure and the space filling volume of each solvent sphere is the same as that for a four-cavity model of *n*-butane. The dash-dot-dash line is for liquid *n*-hexane solvent as calculated with the RISM theory for intermolecular correlations.

$$(\pi/6)\sigma_s^3 = v_{C_4H_{10}}, \quad (4.7)$$

where  $v_{C_4H_{10}}$  is the volume of the four cavity model of *n*-butane. With  $\sigma_{CH_3} = \sigma_{CH_2} = 3.77 \text{ \AA}$ , the calculation of  $v_{C_4H_{10}}$  involves a geometry problem that can be cast as the computation of the third and fourth virial coefficients for a hard sphere gas. The result of the computation yields  $\sigma_s = 5.25 \text{ \AA}$ . The molecular density of the hard sphere fluid,  $\rho_s$ , in the packing fraction theory for the *n*-butane solvent is the density of the *n*-butane solvent at the thermodynamic state under investigation, namely,  $6.05 \times 10^{-3}/\text{\AA}^3$ . The result for  $g_{AA}(r)$  in the hard sphere model solvent was calculated by the procedure detailed in Ref. 3. In that work it was found that the  $g_{AA}(r)$  thus obtained had the accuracy typical of the Percus-Yevick theory applied to hard sphere fluids.<sup>9</sup> From Fig. 4 it is seen that the RISM theory, which accounts for the shape of the *n*-butane molecule and not just its volume, gives a significantly different prediction for  $g_{AA}(r)$  than the simple hard sphere model.

To compare the predictions of the two theories for  $s(\phi)$ , we first calculate the RISM theory result for the cavity distribution. For  $r > \sigma_A$ ,  $y_{AA}(r)$  is given by  $g_{AA}(r)$ . To obtain  $y_{AA}(r)$  inside the hard core we note that for systems which interact with hard core site-site interactions,

$$\ln y_{AA}(0) = \beta \Delta \mu_A$$

$$= -\ln(1 - \xi) + 2\pi\rho_s \sum_{\alpha} \int_0^{\sigma_A} d\sigma g_{A\alpha} \left( \frac{\sigma_{\alpha} + \sigma}{2} \right) \left( \frac{\sigma_{\alpha} + \sigma}{2} \right)^2, \quad (4.8)$$

where  $\xi = \rho_s v_{C_4H_{10}}$  is the packing fraction of the solvent, and  $\Delta \mu_A$  is the excess (interaction) chemical potential for the A particle. Equation (4.8) is perhaps most readily verified by recalling the well known scaled particle theory equation<sup>17</sup>

$$\beta \Delta \mu_A = -\ln(1 - \xi) + \frac{1}{2} \int_0^{\sigma_A} d\sigma P(\sigma), \quad (4.9)$$

where  $P(\sigma)$  is the concentration of atoms in contact with the hard sphere solute of diameter  $\sigma$ . For reference interaction site molecules (hard cores with site-site interactions)

$$P(\sigma) = 4\pi\rho_s \sum_{\alpha} [(\sigma + \sigma_{\alpha})/2]^2 g_{A\alpha}[(\sigma + \sigma_{\alpha})/2]. \quad (4.11)$$

Once  $\beta \Delta \mu_A$  is known then  $\ln y_{AA}(r)$  is calculated as described in Ref. 3. In particular, we write

$$\ln y_{AA}(r) \approx \sum_{n=0}^3 a_n \left( \frac{r - \sigma_A}{\sigma_A} \right)^n \quad r < \sigma_A, \quad (4.12)$$

and the coefficients,  $a_n$ , are fixed by demanding that  $y_{AA}(r)$  and its first two derivatives are continuous, and  $y_{AA}(0)$  is given by Eq. (4.8).

With  $y_{AA}(r)$  thus determined, we compute  $s(\phi)$  from Eq. (2.4) since in the two cavity model  $y^*(\phi) = y_{AA}(r_{xx}[\phi])$ . The results for  $s(\phi)$  are shown in Fig. 5. With this intramolecular distribution and Eq. (2.6) we obtain  $K = (x_g/x_l) \approx 0.664$  for *n*-butane in the neat liquid. On the other hand, using the hard sphere model as described above, and the "exact" hard sphere mixture cavity distribution function (see the Appendix), we obtain  $K \approx 0.859$ .

These values for the equilibrium constant can be compared with the mole fraction ratio obtained by Ryckaert and Bellemans.<sup>5</sup> These workers performed a computer simulation of the four cavity model of *n*-butane we have

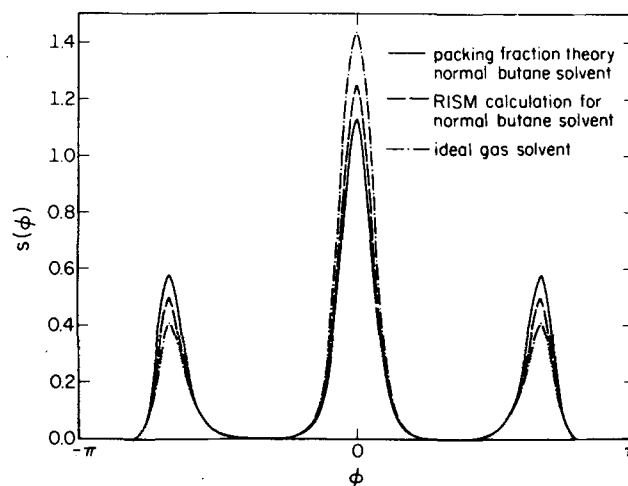


FIG. 5. Intramolecular distribution for *n*-butane at 274 °K. The dash-dot-dash line is appropriate when *n*-butane is in the gas phase. The dashed line is for *n*-butane dissolved in the neat liquid, and the liquid is treated with the RISM theory. The solid line is also for *n*-butane in the neat liquid. But here, the solvent molecules are modeled as simple spheres and the diameter of spheres are chosen so as to obtain objects occupying the same volume as a space filling four-cavity model of *n*-butane (See Table I).



discussed. The intramolecular potential energy is the Scott-Scheraga  $V(\phi)$ . The temperature and density they studied are 274 °K and  $6.05 \times 10^{-3}/\text{\AA}^3$ —the same as we have employed. They report the average intramolecular potential energy per molecule,  $\langle V(\phi) \rangle$ . This single number tells us the value of  $x_g/x_t$  since

$$\begin{aligned} \langle V(\phi) \rangle &= \int_{-\pi}^{\pi} d\phi y^*(\phi) s^{(0)}(\phi) V(\phi) \left( \int_{-\pi}^{\pi} d\phi y^*(\phi) s^{(0)}(\phi) \right)^{-1} \\ &\approx [2y_g^* V_g^{(0)} + y_t^* V_t^{(0)}] / [y_g^* x_g^{(0)} + y_t^* x_t^{(0)}] \\ &= (x_g/x_g^{(0)}) V_g^{(0)} + (x_t/x_t^{(0)}) V_t^{(0)}, \end{aligned} \quad (4.13)$$

where

$$V_g^{(0)} = \int_g d\phi s^{(0)}(\phi) V(\phi), \quad (4.14)$$

and  $V_t^{(0)}$  has a similar definition. [Numerical tests indicate that the approximation in Eq. (4.13) is accurate to better than 2%.] Equation (4.13), the value of  $\langle V(\phi) \rangle$ , and  $x_g + x_t = 1$  can be combined to yield  $(x_g/x_t)$ . The computer simulation result obtained in this way is  $K \approx 0.67$ . The uncertainty is roughly  $\pm 0.01$  judging from the apparent size of the errors in the value for  $\langle V(\phi) \rangle$  reported by Rychaert and Bellemans. The ideal gas  $K$  for this temperature is 0.481.

These numbers indicate that there is indeed a shift of conformational equilibrium from gas phase values even in the absence of electrostatic effects. The phenomenon is a result of the repulsive steric forces which describe the shape of the solvent molecules. The theoretical calculations which employ the RISM equation for the intermolecular structure along with the two cavity model apparently do justice to the steric effects. However, the simple hard sphere or packing fraction theory which replaces the *n*-butane solvent molecules with spheres of the same molecular volume seems to overestimate the size of the steric effects.

The differences between the results obtained with the hard sphere model solvent and with the RISM theory, see Figs. 4 and 5, are interesting. The physical basis for proposing the hard sphere model was the belief that one needs only a realistic description of the volume which the solvent molecules exclude from the cavities in order to understand the effect of steric forces on the intramolecular structure of nonrigid molecules in condensed phases. This excluded volume argument still provides a fundamental explanation of the effect of condensed phases on conformational equilibria. But the results of this section show that for accurate work, one requires a more sophisticated account of the shape of the solvent molecules. Their volume alone is not sufficient to predict  $s(\phi)$  with high accuracy.

One explanation of why the contact value of  $g_{AA}(r)$  obtained with the RISM theory, see Fig. 4, is lower than that obtained from the hard sphere model is the following: With the hard sphere model, the structural oscillations are determined by a single characteristic length—the diameter of the solvent spheres. With the RISM theory, there are several more lengths, namely, the intramolecular site-site separations, which enter the problem. These extra characteristic lengths produce

an interference, and structural features in  $g_{AA}(r)$  are washed out.

In order to examine these ideas we have also used the RISM equation to calculate the cavity distribution function for hard sphere cavities of diameter 4.39 Å, dissolved in liquid *n*-hexane. The model of *n*-hexane adopted for the calculations is the natural extension of the one used for the *n*-butane RISM calculation. Figure 2 shows a drawing of this model *n*-hexane molecule in the completely extended state. This molecule has three conformational degrees of freedom. These are the bond rotations about axes defined by the bonds between sites 2–3, 3–4, and 4–5. See Fig. 2. Because of the extra degrees of freedom, explicit determination of the  $s_{\alpha\gamma}^{(2)}(r)$  is fairly difficult. We therefore investigate a discrete model of the conformational states of *n*-hexane. This is the rotational isomeric model<sup>7</sup> used in Ref. 3. With this model the contracted intramolecular distribution functions are given by

$$\begin{aligned} [s_{\alpha\gamma}^{(2)}(r)]_{\text{discrete model}} \\ = \sum_i x_i [4\pi L_{\alpha\gamma}^2(i)]^{-1} \delta[r - L_{\alpha\gamma}(i)]. \end{aligned} \quad (4.15)$$

Here,  $i$  indexes the possible conformational states of the molecule,  $x_i$  is the mole fraction of molecules in conformational state  $i$ , and  $L_{\alpha\gamma}(i)$  is the length between sites  $\alpha$  and  $\gamma$  when the molecule is in state  $i$ . We have tested this discrete model by comparison of the results obtained with the discrete model and with the continuous model of the intermolecular correlations in pure liquid *n*-butane. We find that  $\hat{s}_{\alpha\gamma}^{(2)}(k)$  is indeed well approximated by  $[\hat{s}_{\alpha\gamma}^{(2)}(k)]_{\text{discrete model}}$ , and as a result the intermolecular correlation functions obtained from the two methods are indistinguishable.

In order to apply Eq. (4.15) we must analyze the allowed conformational states of *n*-hexane. This is straightforwardly accomplished by the methods described in Ref. 3. The methyl sites are taken to be hard spheres with diameter 3.77 Å. Thus, no pair of sites separated by more than three bonds are allowed to approach each other closer than 3.77 Å. The enumeration of allowed states yields  $s_{\alpha\gamma}^{(2)}(r)$  from Eq. (4.15). Once the  $s_{\alpha\gamma}^{(2)}(r)$ 's are formed, the RISM calculation and calculation of the cavity distribution function proceed in entirely the same manner described previously, Eqs. (4.2)–(4.4). The density of *n*-hexane used in the calculation is  $\rho = 4.62 \times 10^{-2}/\text{\AA}^3$ , which is appropriate at 1 atm pressure and  $T = 274^\circ\text{K}$ .<sup>18</sup> Figure 4 shows the  $g_{AA}(r)$  obtained. The cavity distributions are then computed as before and we finally find, for *n*-butane dissolved in *n*-hexane,  $K \approx 0.681$ . This value suggests that the local environment of an *n*-butane solute molecule, in either liquid *n*-butane or liquid *n*-hexane, is much the same.

## V. DISCUSSION

In view of the calculations we have presented, there can be no doubt that nonassociated dense liquids alter the intramolecular distribution function of *n*-butane solute molecules from its gas phase values. The results we have obtained for the ratio  $x_g/x_t$  are summarized in Table II. The standard treatment<sup>4</sup> of conforma-

TABLE II. Summary of conformational equilibrium constants,  $K = x_g/x_l$ , obtained with the various calculations (all at 1 atm total pressure).

Solvent	T(°K)	Approximation method	$x_g/x_l$
Ideal gas	283.2	No approximation	0.502
Liquid CCl <sub>4</sub>	283.2	Hard sphere model solvent; superposition approximation	1.47
Liquid CCl <sub>4</sub>	283.2	Hard sphere model solvent; two cavity model of <i>n</i> -butane-solvent interaction	0.988
Ideal gas	274	No approximation	0.481
Liquid <i>n</i> -butane	274	Hard sphere model solvent; two cavity model of <i>n</i> -butane solvent interaction	0.859
Liquid <i>n</i> -butane	274	RISM theory for solvent; two cavity model of <i>n</i> -butane-solvent interaction	0.664
Liquid <i>n</i> -butane	274	Molecular dynamics calculation of Ryckaert and Bellemans <sup>a</sup>	0.67 ± 0.01 <sup>a</sup>
Liquid <i>n</i> -hexane	274	RISM theory for solvent; two cavity model of <i>n</i> -butane-solvent interaction	0.681

<sup>a</sup>Estimated from numbers given in Ref. 5. See text.

tional equilibrium in condensed phase focuses on the fact that a dielectric medium changes the work required to alter the electric charge distribution of the molecules from that found when the molecule is in the gas phase. The steric contributions to the condensed phase effect are usually ignored.

Measured values of the conformational equilibrium constant,

$$K = x_g/x_l, \quad (5.1)$$

are almost always analyzed by plotting  $\ln K$  vs  $1/T$  at constant pressure. The slope

$$(\partial \ln K / \partial T^{-1})_p = -\Delta H / k_B \quad (5.2)$$

is then taken to be the effective energy difference between the *trans* and *gauche* states. There are several factors which may make such an analysis insensitive to the steric contributions on which we have focused. Since in taking the derivative, Eq. (5.2), both temperature and density are changed, disentanglement of the steric contribution to  $\Delta H$  requires careful treatment. To study this problem quantitatively we first note that for the ideal gas equilibrium constant,  $K^{(0)}$ , it is true that

$$(\partial \ln K^{(0)} / \partial T^{-1})_p = -\Delta H^{(0)} / k_B$$

does yield a  $\Delta H^{(0)}$  which is a good approximation to the energy difference between the *trans* and *gauche* states. This is shown in Fig. 6. The change in  $\ln K^{(0)}$  due to the condensed phase,  $\ln(K/K^{(0)}) \equiv \Delta \ln K$ , is only a very mild explicit function of temperature. It is usually more sensitive to density changes than temperature changes. However, for a temperature change at constant pressure, the density also changes. Thus,

$$\begin{aligned} (\partial \Delta \ln K / \partial T^{-1})_p &= -T^2 [(\partial \Delta \ln K / \partial T)_p \\ &\quad + (\partial \Delta \ln K / \partial \rho)_T (\partial \rho / \partial T)_p] \\ &= -T^2 [(\partial \Delta \ln K / \partial T)_p \\ &\quad - \rho \alpha (\partial \Delta \ln K / \partial \rho)_T]. \end{aligned} \quad (5.3)$$

Here  $\alpha$  is the coefficient of thermal expansion,

$$\alpha = V^{-1}(\partial V / \partial T)_p,$$

and throughout this section  $\rho$  stands for the solvent density,  $\rho_s$ . The first term on the right side of Eq. (5.3) can be estimated by the same methods employed in the discussion of the entropy of apolar solutes in liquid water, Ref. 3. In particular, the ratio  $K/K^{(0)}$  depends on  $T$  at constant solvent density only through the temperature dependence of the hard core diameters,

$$(\partial \Delta \ln K / \partial T)_p = \sum_i (\partial \Delta \ln K / \partial \sigma_i)_p (d\sigma_i / dT),$$

where  $\sigma_i$  denotes the  $i$ th core diameter in the model. In view of the entries in Table I,  $d\sigma_i/dT$  is of the order of  $3 \times 10^{-4} \sigma_i/\text{deg}$ . Further, the cavity distributions tabulated in the Appendix indicate that at typical liquid densities,  $(\partial \Delta \ln K / \partial \sigma_i)_p$  is of the order of  $\sigma_i^{-1}$ . Indeed, explicit evaluation gives

$$(k_B T^2 / \Delta H^{(0)}) (\partial \Delta \ln K / \partial T)_p \approx 0.08.$$

The errors in measurement of liquid state conformational equilibrium are typically<sup>19,20</sup> larger than 10% in  $\Delta H$ . Therefore, it is not surprising that the first factor on the right-hand side of Eq. (5.3) has been neglected. However, the second term may or may not be important, depending on the size of  $\alpha$  and  $(\partial \Delta \ln K / \partial \rho)_T$ . From the functions tabulated in the Appendix we estimate that for *n*-butane in CCl<sub>4</sub>

$$(\partial \Delta \ln K / \partial \rho)_T = 3.8 \times 10^2 \text{ Å}^3.$$

Furthermore, for CCl<sub>4</sub> at 274 °K,<sup>21</sup>

$$\alpha = 1.2 \times 10^{-3} \text{ deg}^{-1},$$

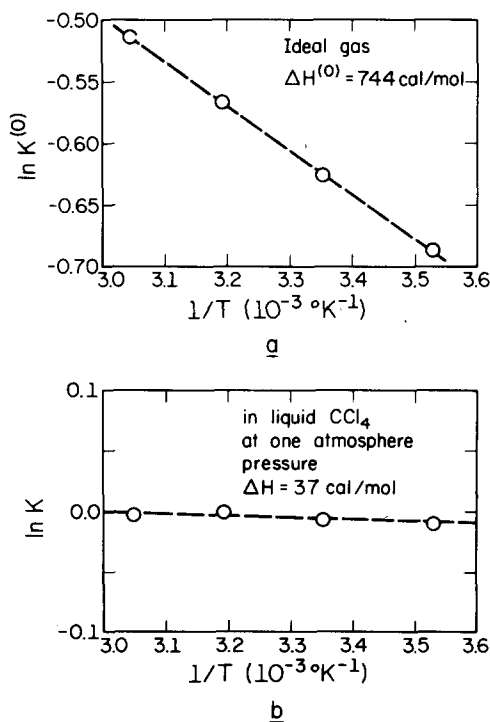


FIG. 6. Arrhenius plot of the *trans*-*gauche* equilibrium constant,  $K = x_g/x_l$ : (a) For *n*-butane in the gas phase; (b) For *n*-butane dissolved in liquid carbon tetrachloride.

so that

$$k_B T^2 \rho \alpha (\partial \ln K / \partial \rho)_T \approx 460 \text{ cal/mole}.$$

Thus, the steric effects will make a significant contribution when data for *n*-butane in  $\text{CCl}_4$  are analyzed by this method.

A contribution as large as 500 cal/mole to a quantity which is of the order 1000 cal/mole is too large to have been lost in experimental error. Therefore, one might wonder why the steric effects which we have calculated have not been identified before. As a step towards resolving this question we note that the analysis of  $(\partial \ln K / \partial T^{-1})_p$  for *n*-butane in  $\text{CCl}_4$  does not seem to correctly describe  $(\partial \ln K / \partial T^{-1})_p$  for *n*-butane in the pure liquid. Verma, Murphy, and Bernstein<sup>19</sup> have measured

$$\Delta H^{(0)} = 966 \text{ cal/mole} \pm 54 \text{ cal/mole}.$$

Furthermore,  $\Delta H$  for *n*-butane in the pure liquid has been measured by Szasz, Sheppard, and Rank.<sup>20</sup> They find

$$\Delta H = 770 \text{ cal/mole} \pm 90 \text{ cal/mole}.$$

Since  $\text{CCl}_4$  is fairly spherical, the analysis of  $K$  for *n*-butane in liquid  $\text{CCl}_4$  seems fairly reliable. However, *n*-butane is not so spherical. We have found in Sec. IV that the assumption that the solvent molecules may be modeled as hard spheres may introduce important errors in the calculation of  $K$ . Thus, one may expect the estimate of the size of  $(\partial \Delta \ln K / \partial \rho)_T$  to be different for liquid *n*-butane than for  $\text{CCl}_4$ . The value of  $(\partial \Delta \ln K / \partial \rho)_T$  may be more accurately estimated by performing RISM calculations, as described in Sec. IV, for a series of densities. By this method we have estimated

$$(\partial \Delta \ln K / \partial \rho)_T \approx 72 \text{ \AA}^3.$$

For *n*-butane,<sup>22</sup>

$$\alpha \approx 2.2 \times 10^{-3} \text{ deg}^{-1};$$

thus,

$$k_B T^2 \rho \alpha (\partial \Delta \ln K / \partial \rho)_T \approx 170 \text{ cal/mole}.$$

This result is in accord with both experimental measurements. This interesting difference between liquid  $\text{CCl}_4$  and liquid *n*-butane as solvents may be physically explained in the following way: In response to a density increase, a liquid composed of aspherical molecules may relieve the induced stress by alteration of orientational correlations as well as by other means, such as tighter packing of molecular centers. Since a hard sphere liquid obviously does not have orientational degrees of freedom only the latter mechanisms are operative. Thus, the assumption that the solvent molecules may be modeled as hard spheres results in an overestimate of  $(\partial \Delta K / \partial \rho)_T$ .

These results clearly indicate that an experimental study of  $K$  for a variety of solvents could reveal differences in  $\Delta H$  which are directly attributable to the steric contribution to  $K$ . They also show that the steric contributions to  $K$  are much more sensitive to changes in density than they are to changes in the temperature with density held constant. Figure 7 shows the results we

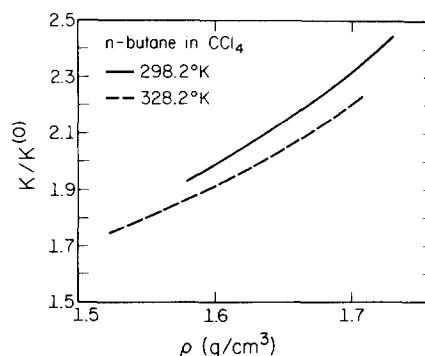


FIG. 7. *Trans-gauche* equilibrium constant  $K$  versus solvent density for *n*-butane in liquid  $\text{CCl}_4$ . At 298.2°K, the slope gives a partial molar volume of reaction to be  $-4.7 \text{ cm}^3/\text{mole}$ .

predict for a study of  $K$  as a function of density at constant temperature. Since McCool and Woolf<sup>12</sup> have measured the equation of state for  $\text{CCl}_4$  in the region pertinent to Fig. 7, we are able to calculate

$$k_B T (\partial \ln K / \partial \rho)_T = [-\Delta V]_{\text{CCl}_4 \text{ solvent}} \approx 4.7 \text{ cm}^3/\text{mole}$$

at 298.2°K. It is interesting to compare this value of  $\Delta V$  for the *trans-gauche* reaction in  $\text{CCl}_4$  solvent with that in the neat liquid. Since

$$k_B T (\partial \ln K / \partial \rho)_T = (\partial \ln K / \partial \rho)_T (\partial \rho / \partial \beta p)_T,$$

the value of  $(\partial \ln K / \partial \rho)_T$  given above for *n*-butane solvent,  $72 \text{ \AA}^3$ , can be combined with an estimate of  $(\partial \rho / \partial \beta p)_T$  for *n*-butane, 0.04, to yield

$$[-\Delta V]_{\text{neat liquid}} \approx 2 \text{ cm}^3/\text{mole},$$

which is significantly smaller than the  $\text{CCl}_4$  solvent result.

In summary, we conclude that the phenomena associated with the steric contribution to  $K$  has been unappreciated largely because experiments have been limited to a small range of solvents and densities. However, we have shown, see Table II, that a variety of approximation methods all establish that the steric contribution to  $K$  is a real physical phenomenon. We have shown that our predictions may be tested by straightforward experimental methods. Thorough experimental study of the problems we have identified may also be expected to shed light on questions regarding re-examination of standard dielectric treatments of conformational equilibria.

## APPENDIX: DISTRIBUTION FUNCTION FOR TWO HARD SPHERE CAVITIES IN A HARD SPHERE SOLVENT

We represent  $y_{\text{HS}}(r; \sigma, \sigma_s; \rho_s)$  for  $r < \sigma$  with an interpolation formula,

$$\ln y_{\text{HS}}(r) = \sum_{n=0}^3 a_n (r - \sigma)^n / \sigma^n, \quad r < \sigma, \quad (\text{A1})$$

where the coefficients  $a_n$  are fixed from the knowledge of the following:

TABLE III. Coefficients to determine the distribution function for two hard sphere cavities of diameter  $\sigma$  dissolved at infinite dilution in a solvent of hard spheres with diameter  $\sigma_S$  at a density  $\rho_S$ .

$\rho_S \sigma_S^3$	$\sigma/\sigma_S$	$a_0$	$a_1$	$a_2$	$a_3$
0.70	0.40	0.77420	-0.91290	0.13568	0.04308
	0.50	0.84571	-1.26060	0.40340	0.15118
	0.60	0.91457	-1.64716	0.81974	0.32013
	0.70	0.98097	-2.06897	1.41062	0.56013
	0.80	1.04510	-2.52308	2.20083	0.88078
	0.90	1.10711	-3.00691	3.21435	1.29133
	1.00	1.16714	-3.51826	4.47459	1.80071
	1.20	1.28178	-4.61570	7.82668	3.15073
	1.40	1.38990	-5.80154	12.43710	4.99893
	1.60	1.49222	-7.06403	18.48206	7.41159
	1.80	1.58937	-8.39299	26.13500	10.45366
	2.00	1.68184	-9.77951	35.56709	14.18899
0.75	0.40	0.85039	-1.05593	0.16573	0.05119
	0.50	0.92872	-1.45598	0.49976	0.18577
	0.60	1.00388	-1.89956	1.01897	0.39622
	0.70	1.07613	-2.38230	1.75548	0.69516
	0.80	1.14571	-2.90059	2.74003	1.09456
	0.90	1.21280	-3.45131	4.00243	1.60591
	1.00	1.27760	-4.03174	5.57174	2.24038
	1.20	1.40092	-5.27228	9.74493	3.92207
	1.40	1.51674	-6.60536	15.48344	6.22463
	1.60	1.62597	-8.01686	23.00626	9.23075
	1.80	1.72933	-9.49471	32.52876	13.02139
	2.00	1.82744	-11.02851	44.26333	17.67605
0.80	0.40	0.93081	-1.21998	0.20298	0.06088
	0.50	1.01627	-1.67930	0.61949	0.22823
	0.60	1.09798	-2.18709	1.26658	0.49003
	0.70	1.17627	-2.73807	2.18405	0.86196
	0.80	1.25144	-3.32783	3.41005	1.35890
	0.90	1.32374	-3.95259	4.98158	1.99517
	1.00	1.39338	-4.60905	6.93477	2.78468
	1.20	1.52546	-6.00563	12.12755	4.87752
	1.40	1.64901	-7.49737	19.26643	7.74335
	1.60	1.76510	-9.06755	28.62325	11.48515
	1.80	1.87461	-10.70212	40.46506	16.20359
	2.00	1.97826	-12.38921	55.05507	21.99748
0.85	0.40	1.01589	-1.40911	0.24957	0.07258
	0.50	1.10881	-1.93576	0.75924	0.28068
	0.60	1.19734	-2.51606	1.57614	0.60638
	0.70	1.28188	-3.14360	2.71966	1.06915
	0.80	1.36280	-3.81304	4.24714	1.68751
	0.90	1.44040	-4.51982	6.20458	2.47930
	1.00	1.51497	-5.25996	8.63687	3.46183
	1.20	1.65591	-6.82663	15.10174	6.06657
	1.40	1.78720	-8.48911	23.98703	9.63360
	1.60	1.91013	-10.22796	35.63004	14.29101
	1.80	2.02573	-12.02715	50.36190	20.16388
	2.00	2.13483	-13.87340	68.50885	27.37496
0.90	0.40	1.10614	-1.62839	0.30846	0.08690
	0.50	1.20689	-2.23180	0.95794	0.34600
	0.60	1.30251	-2.89421	1.96579	0.75168
	0.70	1.39351	-3.60785	3.39335	1.32816
	0.80	1.48034	-4.36627	5.29952	2.09852
	0.90	1.56339	-5.16399	7.74149	3.08497
	1.00	1.64297	-5.99626	10.77513	4.30911
	1.20	1.79286	-7.74827	18.83587	7.55442
	1.40	1.93192	-9.59435	29.91083	11.99864
	1.60	2.06167	-11.51225	44.41889	17.80106
	1.80	2.18329	-13.48405	62.77115	25.11722
	2.00	2.29776	-15.49525	85.37257	34.09970

TABLE III (Continued)

$\rho_S \sigma_S^3$	$\sigma/\sigma_S$	$a_0$	$a_1$	$a_2$	$a_3$
0.95	0.40	1.20214	-1.88423	0.38370	0.10472
	0.50	1.31112	-2.57552	1.19775	0.42809
	0.60	1.41413	-3.33119	2.46005	0.93457
	0.70	1.51183	-4.14188	4.24700	1.65435
	0.80	1.60474	-4.99982	6.63202	2.61620
	0.90	1.69335	-5.89849	9.68639	3.84786
	1.00	1.77803	-6.83228	13.47971	5.37626
	1.20	1.93698	-8.78629	23.55529	9.42795
	1.40	2.08385	-10.82970	37.39297	14.97588
	1.60	2.22038	-12.93751	55.51407	22.21843
	1.80	2.34797	-15.09014	78.43023	31.34937
	2.00	2.46774	-17.27211	106.64560	42.55881

$$(i) \ y_{HS}(0; \sigma, \sigma_S; \rho_S),$$

$$(ii) \ y'_{HS}(0; \sigma, \sigma_S; \rho_S),$$

$$(iii) \ y_{HS}(\sigma; \sigma, \sigma_S; \rho_S),$$

and

$$(iv) \ y'_{HS}(\sigma; \sigma, \sigma_S; \rho_S).$$

The primes in Items (ii) and (iv) indicate first derivatives. Grundke and Henderson<sup>13</sup> proposed such an interpolation formula, and Torrie and Patey<sup>23</sup> have found that it is a very accurate procedure when  $\sigma = \sigma_S$ . When  $\sigma \neq \sigma_S$ ,  $y_{HS}(r; \sigma, \sigma_S; \rho_S)$  is a cavity distribution for a hard sphere mixture in which the solute particles with diameter  $\sigma$  are at *infinite dilution*. Unfortunately, the procedure developed by Grundke and Henderson to calculate Item (iv) for mixtures fails in the limit of infinite dilution. Hence, to apply the interpolation formula, Eq. (A1), another procedure is needed. The method we have devised is outlined now.

We make a literal extension of the method proposed by Verlet and Weis<sup>24</sup> in their study of pure hard sphere fluids. First, for  $r > \sigma$ ,  $y_{HS}(r)$  is represented as a phase shifted Percus-Yevick (PY) cavity distribution<sup>25</sup> plus a correction:

$$y_{HS}(r; \sigma, \sigma_S; \rho_S \sigma_S^3) = [y_{HS}(r; \bar{\sigma}, \bar{\sigma}_S; \rho_S \sigma_S^3)]_{PY} + \frac{A}{r} \bar{e}^{\mu(r-\sigma)} \cos[\mu(r-\sigma)] \quad r > \sigma, \quad (A2)$$

where

$$\bar{\sigma} = \sigma f, \quad \bar{\sigma}_S = \sigma_S f, \quad (A3a)$$

with

$$f = [1 - (1/16)(\pi/6)\rho_S \sigma_S^3]^{1/3}. \quad (A3b)$$

The contact value, Item (iii), and the slope at  $r=0$ , (Item ii), are determined by assuming they are given by  $\frac{1}{3}$  the Percus-Yevick values plus  $\frac{2}{3}$  the scaled particle theory values. This is consistent with the Mansoori equation of state.<sup>26</sup> Item (iii) fixes the parameter  $A$  in Eq. (A2). The Mansoori equation of state also determines Item (i). To find the slope of  $y_{HS}(r)$  at  $r=\sigma$ , Item (iv), we must fix the parameter  $\mu$  in Eq. (A2). This is done by fixing the area under  $y_{HS}(r) - 1$  for  $r > \sigma$  in the same manner as proposed by Verlet and Weis<sup>24</sup> when they considered the one-component fluid. In particular, we assume

$$\int_0^\sigma dr r^2 [y_{HS}(r; \bar{\sigma}, \bar{\sigma}_S)]_{PY} = \int_0^\infty dr r^2 \Delta y_{HS}(r), \quad (A4)$$

where  $\Delta y_{HS}(r)$  stands for the second term on the right hand side of Eq. (A2). After performing the integrations, Eq. (A4) leads to a formula for  $\mu$  that is similar to Eq. (2.17) of Ref. 24. Table III lists the coefficients  $a_n$  calculated by this method for several densities and diameters.

<sup>1</sup>D. Chandler and L. R. Pratt, J. Chem. Phys. **65**, 2925 (1976).

<sup>2</sup>L. R. Pratt and D. Chandler, J. Chem. Phys. **66**, 147 (1977).

<sup>3</sup>L. R. Pratt and D. Chandler, J. Chem. Phys. **67**, 3683 (1977).

<sup>4</sup>R. J. Abraham and E. Bretschneider, in *Internal Rotation in Molecules*, edited by W. J. Orville-Thomas (Wiley, New York, 1974).

<sup>5</sup>J.-P. Ryckaert and A. Bellemans, Chem. Phys. Lett. **30**, 123 (1975).

<sup>6</sup>D. Chandler and H. C. Andersen, J. Chem. Phys. **57**, 1930 (1972); D. Chandler, J. Chem. Phys. **59**, 2749 (1973); D. Chandler, Mol. Phys. **31**, 1213 (1976).

<sup>7</sup>P. J. Flory, *Statistical Mechanics of Chain Molecules* (Interscience, New York, 1969).

<sup>8</sup>R. A. Scott and H. A. Scheraga, J. Chem. Phys. **44**, 3054 (1966).

<sup>9</sup>J. P. Hansen and I. R. McDonald, *Theory of Simple Liquids* (Academic, New York, 1976).

<sup>10</sup>H. C. Andersen, D. Chandler, and J. D. Weeks, Adv. Chem. Phys. **34**, 105 (1976).

<sup>11</sup>D. Chandler, J. Chem. Phys. **62**, 1358 (1975).

<sup>12</sup>M. A. McCool and L. A. Woolf, Chem. Soc. Faraday Trans. **1** **68**, 1971 (1972).

<sup>13</sup>E. W. Grundke and D. Henderson, Mol. Phys. **24**, 269 (1972).

<sup>14</sup>L. J. Lowden and D. Chandler, J. Chem. Phys. **61**, 5228 (1974); C. S. Hsu, D. Chandler, and L. J. Lowden, Chem. Phys. **14**, 213 (1976); D. Chandler, C. S. Hsu, and W. B. Streett, J. Chem. Phys. **66**, 5231 (1977).

<sup>15</sup>L. J. Lowden, RISM, RISMGR, RISMSK; Program number QCPE 306; Quantum Chemistry Program Exchange, Indiana University, Bloomington, IN 47401.

<sup>16</sup>C. S. Hsu, L. R. Pratt, and D. Chandler, J. Chem. Phys. **68**, 4213 (1978), following article.

<sup>17</sup>H. Reiss, Adv. Chem. Phys. **9**, 1 (1965); H. Reiss, in *Statistical Mechanics and Statistical Methods in Theory and Application*, edited by U. Landman (Plenum, New York, 1977).

<sup>18</sup>*Handbook of Chemistry and Physics 50th Edition*, edited by R. C. Weast (Chemical Rubber Co., Cleveland, OH, 1969).

<sup>19</sup>A. L. Verma, W. F. Murphy, and H. J. Bernstein, J. Chem. Phys. **60**, 1540 (1974).

<sup>20</sup>G. J. Szasz, N. Sheppard, and D. H. Rank, J. Chem. Phys. **16**, 704 (1948).

<sup>21</sup>J. S. Rowlinson, *Liquids and Liquid Mixtures* (Butterworth, London, 1969).

<sup>22</sup>*International Critical Tables*, edited by E. W. Washburn (McGraw-Hill, London, 1928), Vol. 3, p. 27.

<sup>23</sup>G. Torrie and G. N. Patey, Mol. Phys. **34**, 1623 (1977).

<sup>24</sup>L. Verlet and J.-J. Weis, Phys. Rev. A **5**, 939 (1972).

<sup>25</sup>J. L. Lebowitz, Phys. Rev. Sect. A **133**, 895 (1964).

<sup>26</sup>G. A. Mansoori, N. F. Carnahan, K. E. Starling, and T. W. Leland, Jr., J. Chem. Phys. **54**, 1523 (1971).